Reduction of Voltage Harmonics in an Open-End Winding Induction Motor Driven by a Dual-Inverter with Floating-Capacitor in the Low-Speed Region

Akihito Mizukoshi
Department of Electrical, Electronics and Information Engineering
Nagaoka University of Technology
Nagaoka, Japan
akihito_mizukoshi@stn.nagaokaut.ac.jp

Hitoshi Haga
Department of Electrical, Electronics and Information Engineering
Nagaoka University of Technology
Nagaoka, Japan
hagah@vos.nagaokaut.ac.jp

***Abstract*—A control method to reduce the voltage harmonics in an induction motor is proposed in this paper. This study aims to reduce the carrier harmonics, especially caused by the inverter switching in the low-speed region. The system consists of an open-end winding induction motor (OEWIM) and two voltage-source inverters (VSIs); the dual-inverter is powered by a single DC voltage source and has a capacitor bank. The motor losses, which are caused by the harmonics of the voltage applying to the winding, increase when the inverter outputs a pulse-width modulated (PWM) voltage at a low modulation index. In the proposed method, the use of the output voltage difference between the inverters constituting the dual-inverter lowers the harmonics by keeping the modulation index at high value in each inverter. The theoretical analysis indicates that when the OEWIM is driven at the low-speed condition in the case of using sinusoidal PWM, the voltage total harmonic distortion (THD) can be reduced compared with the single-inverter drive. The performance of the proposed method is simulated and experimentally verified. The results show that the voltage THD of the motor winding are reduced in the low-speed region by 13.9 % at a fundamental frequency of 10 Hz.**

Keywords— Open-end winding induction motor (OEWIM), dual-inverter, floating capacitor.

I. INTRODUCTION

Motor drive systems with high-efficiency operation are required not only at a rated speed, but also in a wide speed range. Various approaches are being pursued to increase the motor efficiency. Multilevel inverters are an effective solution for improving the efficiency of motor drive systems [1]. Since the multilevel inverter outputs a stair-step output voltage, the harmonic components of the output voltage are smaller than those of the output voltage of a 2-level inverter. Another approach to improving the motor efficiency is to reduce the peak value of the pulse-width modulated (PWM) voltage by using a DC/DC converter [2].

Dual-inverter fed open-end winding (OEW) motor topologies and their modulation strategies are been researched for several purposes such as multilevel operations [3]-[6], wide speed range operations [7]-[9], fault-tolerant functions [10]-[11]. In particular, the dual-inverter topology, which has a single power supply and a floating capacitor (FC) in each inverter, can generate a five-level waveform in the winding phase voltage by keeping each DC-link voltage in a ratio of 2:1 [5]-[6]. Through these researches, motor drive systems achieve a high efficiency at rated speed, in other words high modulation index, due to reducing voltage harmonics. A problem focused on this paper is that: when the motor is driven at low-speed, the carrier losses of the motor increase, because the harmonic component of the switching frequency increases compared with the fundamental component [12]. Thus the reduction of the voltage harmonic distortion in the low-speed region is effective for an energy-saving.

The authors have been working on a waveform improvement method that focuses on the low-speed region to reduce the peak voltage of motor winding by using dual-inverter [13]-[14]. Through these works, it has been confirmed that the harmonic component of switching frequency can be reduced by outputting a synchronized PWM waveform in each inverter, when the dual-inverter supplied by two isolated DC voltage sources. The result indicates that the voltage harmonics can be reduced by keeping modulation indices of each inverters at high and keeping a phase difference between two inverters at low. However, the system requires two isolated DC voltage sources.

In this paper, a control method for improving the voltage waveform in the low-speed region is proposed. The dual-inverter is powered by a single DC voltage source, and another inverter only has a capacitor bank. Furthermore, in this paper, an operating condition, that allows to reduce the THD of the phase voltage of motor winding, when the IM driven by the dual-inverter and the single-inverter with sinusoidal PWM (SPWM) is theoretically described. The theoretical analysis indicates that when the OEWIM is driven at the low-speed condition, the voltage THD can be reduced compared with the single-inverter drive. The performance of the proposed control method is simulated and is demonstrated by experiment using an open-ended winding induction motor.

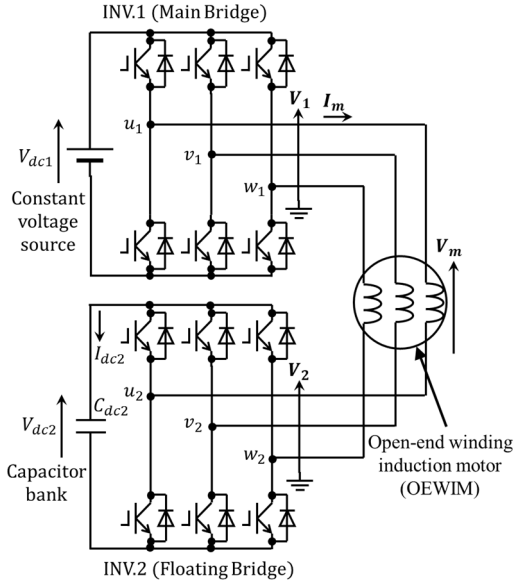

Fig. 1. The configuration of dual inverter fed open-end winding induction motor.

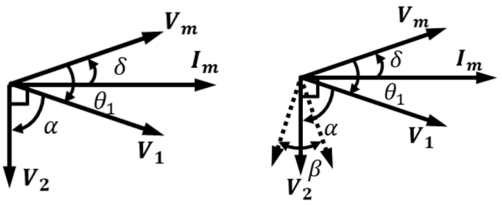

(a) (b)

Fig. 2. Vector diagram of the dual-inverter (a) at steady-state and (b) at transient-state.

TABLE I. VOLTAGE VECTORS AND PHASE VOLTAGE

System	Phase voltage
Single-inverter 8 vectors	$\pm\frac{2}{3}V_{dc1}, \pm\frac{1}{3}V_{dc1}, 0$
Dual-inverter 64 vector combinations	$\pm\frac{2}{3}V_{dc1}, \pm\frac{1}{3}V_{dc1}, \pm\frac{2}{3}V_{dc2}, \pm\frac{1}{3}V_{dc2}$ $\pm\frac{2}{3}(V_{dc1} \pm V_{dc2}), \pm\frac{1}{3}(V_{dc1} \pm V_{dc2}), 0,$ $\pm\frac{1}{3}(2V_{dc1} \pm V_{dc2}), \pm\frac{1}{3}(V_{dc1} \pm 2V_{dc2})$

II. DUAL-INVERTER FED OEWIM WITH AN FC BRIDGE

The configuration of the dual-inverter with a floating capacitor for an open-end winding induction motor is shown in Fig. 1. The system consists of an OEWIM and two 2-level voltage source inverters (VSIs), which are connected to the opposite terminals of the winding, and the dual-inverter is powered by a single DC voltage source. In this work, the main bridge (INV. 1) has a DC power supply and the floating bridge (INV. 2) has a capacitor bank. The output voltage difference between the inverters is supplied to the stator windings in the dual-inverter. Thus, the motor voltage $\boldsymbol{V_m}$ is expressed as follows:

$$\boldsymbol{V_m} = \boldsymbol{V_1} - \boldsymbol{V_2} \tag{1}$$

Here, $\boldsymbol{V_1}$ and $\boldsymbol{V_2}$ are the output voltages of INV. 1 and INV. 2, respectively. Fig. 2 shows the vector diagrams of the dual-inverter and indicates the relationship between $\boldsymbol{V_m}$, $\boldsymbol{V_1}$, and $\boldsymbol{V_2}$. Here, α denotes the phase angle difference between the inverters, and δ denotes the motor power factor angle. Because INV. 2 has no power supply, $\boldsymbol{V_2}$ lags the motor phase current $\boldsymbol{I_m}$ by $\pi/2$ at the steady-state. At the transient-state, that is during the charging or discharging of the INV. 2 capacitor, $\boldsymbol{V_2}$ lags $\boldsymbol{I_m}$ by $(\pi/2 - \beta)$. When β is positive, the capacitor is charged, and when β is negative, the capacitor is discharged. Furthermore, the capacitor is neither charged nor discharged when $\beta = 0$ at the steady-state.

Each 2-level VSIs have 8 switching states, thus the number of switching states in the dual-inverter system becomes 64, and those of phase voltage are shown in Table 1. In the conventional PWM control method of the dual-inverter at low-speed condition, the dual-inverter uses only INV. 1. In this paper, it is called single-inverter operation. A problem of the conventional PWM control method is that, the winding voltage distortion increases because the peak voltage of PWM is fixed at $2V_{dc1}/3$. Therefore, the voltage harmonics caused by the PWM switching increase compared with the fundamental component.

III. THEORETICAL ANALYSIS OF VOLTAGE HARMONICS

A. Voltage RMS and THD Calculation

An RMS value of a PWM voltage is calculated by sum of squared voltage vector V_x^2 multiplied by its outputting time T_x, and subscript x indicates the vector numbers:

$$V_{RMS} = \sqrt{\frac{1}{T}\sum_{x=0}^{N} V_x^2 T_x} \tag{2}$$

The voltage RMS value includes fundamental and all harmonic components, thus the total harmonic distortion (THD) is defined as follows by using fundamental voltage V_F:

$$V_{THD} = \sqrt{\frac{V_{RMS}^2}{V_F^2} - 1} \tag{3}$$

In the case of using dual-inverter and an SPWM, the voltage THD is calculated by equations (2) and (3) as follows:

$$V_{THD,dual} = \sqrt{\frac{8}{\sqrt{3}\pi M}\frac{1 + \left(\frac{V_{dc2}}{V_{dc1}}\right)^2 - \sqrt{\frac{28}{3}}\frac{V_{dc2}}{V_{dc1}}\cos\varphi}{1 + \left(\frac{V_{dc2}}{V_{dc1}}\right)^2 - 2\frac{V_{dc2}}{V_{dc1}}\cos\alpha} - 1} \tag{4}$$

$$\varphi = \frac{\alpha}{2} + \mathrm{Tan}^{-1}\left(\frac{2}{\sqrt{3}}\right) \tag{5}$$

$$V_{F,dual} = \frac{V_{dc1}M}{2\sqrt{2}}\left\{1 + \left(\frac{V_{dc2}}{V_{dc1}}\right)^2 - \frac{V_{dc2}}{V_{dc1}}\cos\alpha\right\} \tag{6}$$

Furthermore the fundamental voltage $V_{F,dual}$ is given by defining the voltage references as follows:

$$\begin{cases} v_{u1} = \dfrac{MV_{dc1}}{2}\cos(\omega t) \\ v_{v1} = \dfrac{MV_{dc1}}{2}\cos\left(\omega t - \dfrac{2}{3}\pi\right) \\ v_{w1} = \dfrac{MV_{dc1}}{2}\cos\left(\omega t + \dfrac{2}{3}\pi\right) \end{cases} \quad \begin{cases} v_{u2} = \dfrac{MV_{dc2}}{2}\cos(\omega t - \alpha) \\ v_{v2} = \dfrac{MV_{dc2}}{2}\cos\left(\omega t - \dfrac{2}{3}\pi - \alpha\right) \\ v_{w2} = \dfrac{MV_{dc2}}{2}\cos\left(\omega t + \dfrac{2}{3}\pi - \alpha\right) \end{cases} \tag{7}$$

Here, α is the phase angle difference between INV.1 and INV.2, and V_{dc2} is the FC voltage. Note that modulation-indices of each inverter have the same value M in this paper.

As well as the THD value and fundamental voltage V_F driven by the single-inverter with SPWM are calculated by $V_{dc2} = 0$ into equations (4) and (6) as follows:

$$V_{THD,single} = \sqrt{\frac{8}{\sqrt{3}\pi M} - 1} \tag{8}$$

$$V_{F,single} = V_{dc1}\frac{M}{2\sqrt{2}} \tag{9}$$

From equation (8), $V_{THD,single}$ can be lower by setting M at high value when V_{dc1} is constant. However, the fundamental voltage $V_{F,single}$ depends on M, thus the THD value becomes relatively high under the low fundamental voltage required. On the other hand as using dual-inverter, from equation (4), $V_{THD,dual}$ can be reduced compared with the single-inverter by changing α and V_{dc2} even when the fundamental voltage is low.

B. *Characteristic of Voltage THD*

In the dual-inverter with the FC bridge, there is relationship between V_{dc2}/V_{dc1}, δ and α, expressed as follows, which is introduced in [7] (see Fig. 2):

$$\frac{V_{dc2}}{V_{dc1}} = \frac{\cos(\alpha - \delta)}{\cos\delta} \tag{10}$$

Therefore, a characteristic of the THD value with respect to fundamental voltage V_F and PFA δ can be theoretically calculated by changing α and V_{dc2} according to following equation and (10):

$$\alpha = \mathrm{Sin}^{-1}\left(\frac{2\sqrt{2}V_F}{MV_{dc1}}\cos\delta\right) \tag{11}$$

Theoretical calculation of voltage THD is carried out in order to clarify a condition, which allows reducing the voltage THD by using dual-inverter compared with the single-inverter drive, as shown in Fig. 3. Here, 1 p.u. of fundamental voltage indicates the inverter outputs a voltage of $V_{dc1}/2\sqrt{2}$, which is a maximum voltage in the single-inverter. Fig. 3 indicates that the voltage THD can be reduced in a condition when the dual-inverter operates at a low fundamental voltage and a large PFA compared with single-inverter drive.

IV. Proposed Control for Reducing the Voltage Harmonics

A proposed control system for reducing the voltage harmonics is shown in Fig. 4. From previous researches [13]-[14], it was confirmed that voltage harmonics can be reduced by outputting a synchronized voltage from each inverter and by keeping the modulation index high in the motor low-speed region where the fundamental component of the output voltage is small. The concept of the proposed control method is described as follows; The required motor voltage

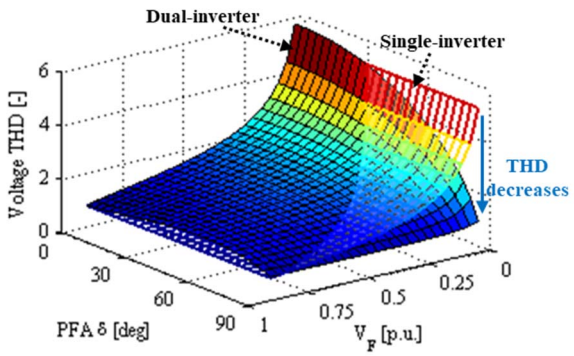

Fig. 3. Theoretical analysis of voltage THD for different fundamental voltage V_F and PFA δ.

$\boldsymbol{V_m} = [v_{dm}\ v_{qm}]^T$ is given by PI controller of the motor current $\boldsymbol{I_m} = [i_{dm}\ i_{qm}]^T$. In order to setting M any value, INV.1 voltage $\boldsymbol{V_1} = [v_{d1}\ v_{q1}]^T$ is calculated as follows: rotating the unit vector of $\boldsymbol{V_m}$ by θ_1 and multiplied by the amplitude of $\boldsymbol{V_1}$ $(= MV_{dc1}/2)$.

$$\boldsymbol{V_1} = \frac{M}{2}V_{dc1}\boldsymbol{T}(\theta_1)\frac{\boldsymbol{V_m}}{|\boldsymbol{V_m}|} \tag{12}$$

$$\boldsymbol{T}(\theta_1) = \begin{bmatrix}\cos\theta_1 & \sin\theta_1 \\ -\sin\theta_1 & \cos\theta_1\end{bmatrix} \tag{13}$$

$$\theta_1 = \alpha + \beta - \delta - \frac{\pi}{2} \tag{14}$$

where θ_1 is phase difference between $\boldsymbol{V_m}$ and $\boldsymbol{V_1}$, and is given by (14). From a relationship between $|\boldsymbol{V_m}|$, $|\boldsymbol{V_1}|$, and $|\boldsymbol{V_2}|$ and (10) (see Fig. 2), α is expressed as follows:

$$\alpha = \frac{1}{2}\mathrm{Cos}^{-1}\left\{1 - 2\left(\frac{|\boldsymbol{V_m}|}{|\boldsymbol{V_1}|}\cos\delta\right)^2\right\} \tag{15}$$

$$\delta = \mathrm{Tan}^{-1}\left(\frac{v_{qm}}{v_{dm}}\right) - \mathrm{Tan}^{-1}\left(\frac{i_{qm}}{i_{dm}}\right) \tag{16}$$

Here, δ denotes the PFA and is calculated by (16). Furthermore, β is given by a PI controller of FC voltage V_{dc2}, while the FC voltage reference V_{dc2}^{ref} is calculated by equation (10). In this system, by ignoring switching and conduction losses, an active power of INV. 2 is expressed as follows [15]:

$$V_{dc2}I_{dc2} = 3|\boldsymbol{V_2}||\boldsymbol{I_m}|\sin\beta \tag{17}$$

Here, amplitude of $\boldsymbol{V_2}$ is defined as $MV_{dc2}/2$ thus,

$$I_{dc2} = \frac{3}{4}M|\boldsymbol{I_m}|\sin\beta \tag{18}$$

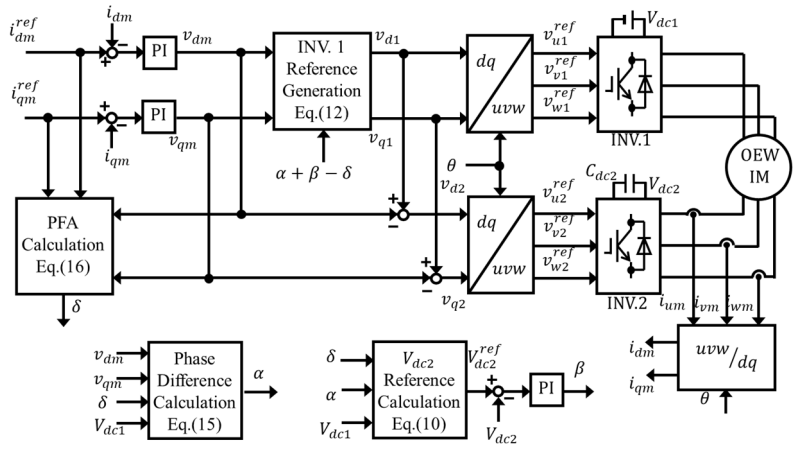

Fig. 4. Proposed control system.

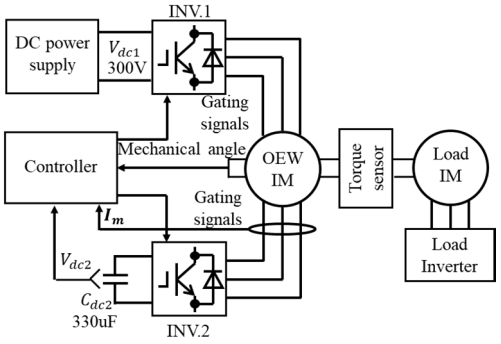

Fig. 5. Experimental setup.

TABLE II. INVERTER CONDITIONS

INV.1 DC Voltage: V_{dc1}	300 V
INV.2 Capacitance: C_{dc2}	330 uF
Fundamental Frequency: f_1	10 Hz to 50 Hz
Carrier Frequency: f_{c1}	5 kHz
Dead-time: T_d	1 us

TABLE III. OEWIM PARAMETERS

Rated power	750 W	Poles	4
Rated voltage	200 V	Rated frequency	50 Hz
Rated current	3.5 A	Rated speed	1410 rpm
Stator resistance R_s	2.74 Ω	Leakage inductance l_s, l_r	10.5 mH
Rotor resistance R_r	2.08 Ω	Mutual inductance L_m	0.195 H

From equation (18), the PI controller of FC voltage is designed depending on the modulation index M and the amplitude of the motor current $|\boldsymbol{I_m}|$.

Finally, the INV. 2 voltage references v_{d2} and v_{q2} are calculated by equation (1). Furthermore, angle θ used for dq-axis transformation is obtained by the slop-frequency type field-oriented control in the proposed method.

V. EXPERIMENTAL SETUP

Experimental conditions and parameters of the OEWIM are shown in Table 2-3. A general-purpose induction motor (TFO-FK 0.75KW 4P 200V, made by HITACHI) is used for experiment. In this experiment, a DC power supply regulates the INV. 1 DC voltage at 300 V, while INV. 2 has a capacitance of 330 uF. Fig. 5 shows an experimental setup. Motor currents, an FC voltage, and a mechanical angle are measured for controlling the motor and the dual-inverter. The slip-frequency type field-oriented control is used in order to keep the fundamental component of the output voltage

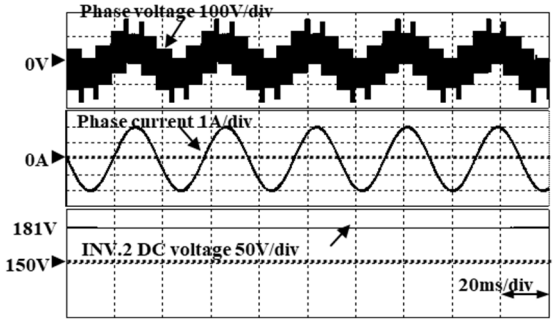

(a)

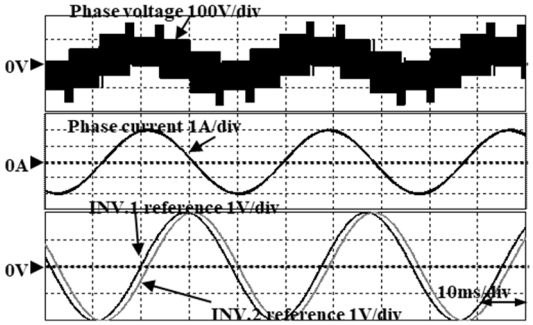

(b)

Fig. 6. Simulated waveforms of the phase voltage, current and (a) capacitor voltage V_{dc2}, (b) INV. 1 and INV. 2 voltage references, when the motor speed is 750rpm with the proposed control.

constant in either case of using dual-inverter or single-inverter. For the verification of the proposed method, the OEWIM is driven at a constant speed from 10 Hz to 50 Hz of fundamental frequency by the load motor. The motor current RMS is regulated at 0.1 p.u. and 0.2 p.u. In the single-inverter operation, OEWIM is driven by only INV. 1, while INV. 2 outputs a zero vector.

VI. SIMULATION AND EXPERIMENTAL RESULTS

A. Performance of the proposed method

Firstly, the performance of the proposed control was verified by simulation. Fig. 6 shows the simulation results of the phase voltage, phase current, capacitor voltage, and INV. 1 and INV. 2 voltage references at a motor speed of 750 rpm. It is confirmed that the capacitor voltage was kept constant

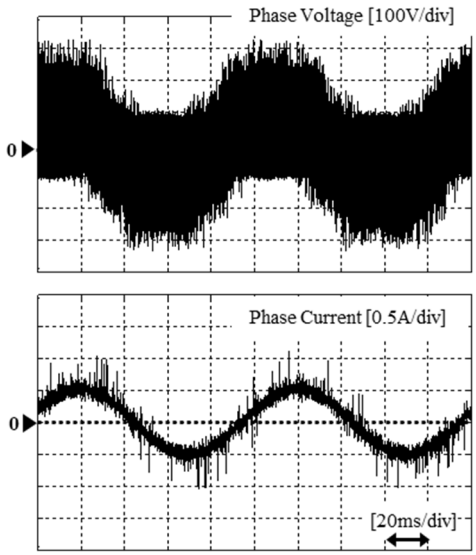

Fig. 7. U-phase voltage and current waveforms with single-inverter, when the OEWIM is driven at 10 Hz of f_1 and 0.1 p.u. of phase current.

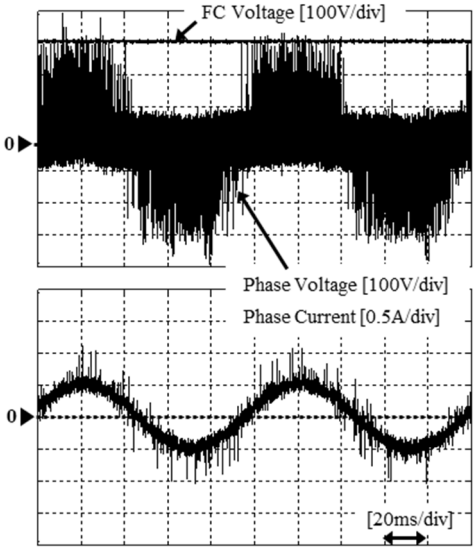

Fig. 8. U-phase voltage and current waveforms with dual-inverter, when the OEWIM is driven at 10 Hz of f_1 and 0.1 p.u. of phase current.

and the modulation index of each inverter was kept at 1. In addition, the FC voltage is regulated at constant voltage.

B. Harmonics Analysis

Fig. 7 and Fig. 8 show U-phase voltage and current waveforms with single-inverter and dual-inverter, when the OEWIM is driven at a fundamental frequency of 10 Hz and a current RMS of 0.1 p.u. Current waveforms indicate that the proposed current control is achieved as well as the single-inverter operation.

Harmonics analysis of the U-phase voltage is carried out under the same condition as shown in Fig. 9. In the case of single-inverter drive, harmonic components, especially integer multiple of carrier frequency 5 kHz, appear at approximately the same value as fundamental component. On the other hand, using dual-inverter with proposed operation, these harmonic components are reduced. Furthermore, it is confirmed that the voltage THD is reduced by 8.91 to 7.67 (-13.9 %).

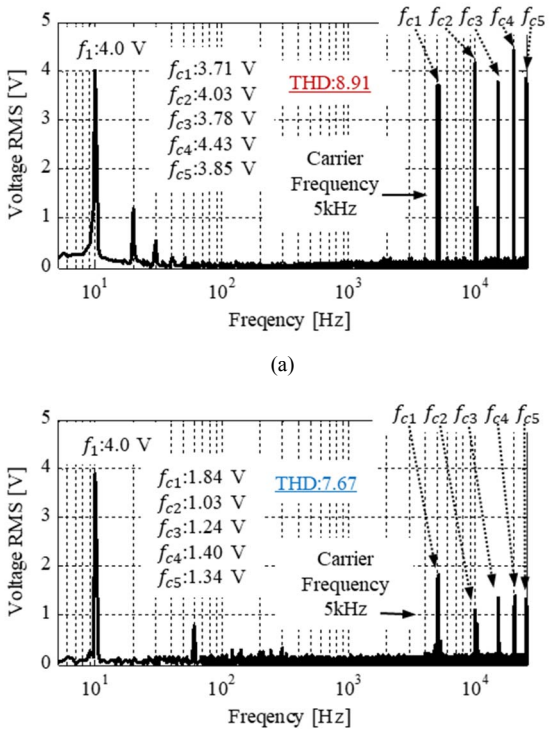

Fig. 9. Harmonics analysis of the U-phase voltage (a) with single-inverter and (b) with dual-inverter at 10 Hz of f_1 and 0.1 p.u. of phase current.

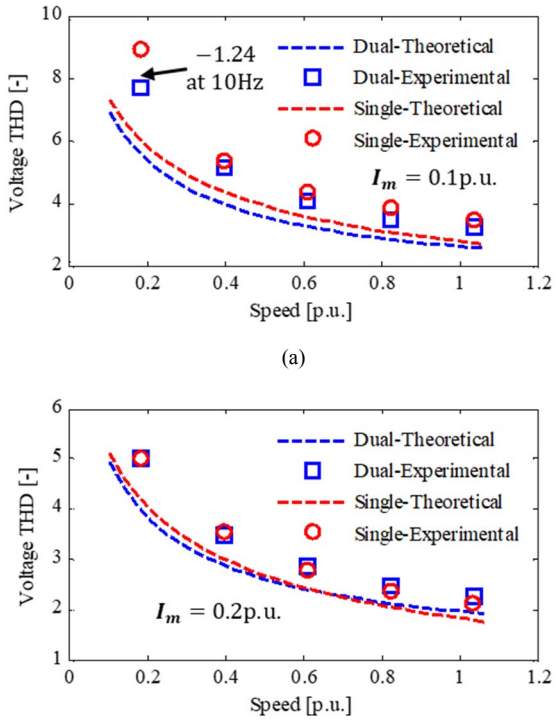

Fig. 10. THD characteristics for different motor speeds when the phase current RMS regulated at (a) 0.1 p.u. and (b) 0.2 p.u.

C. THD Characteristic for Difference Motor Speed

The voltage THD for different speed under the constant current reference are obtained. Fig. 14 shows the THD characteristics when the phase current RMS regulated at (a) 0.1 p.u. and (b) 0.2 p.u. Here, the theoretical lines are

calculated by equations (4) and (8) with considering the relationship of V_F and δ. In addition, the experimental results of THD is given by measuring the voltage RMS and the fundamental component and according to equation (3). Theoretical and experimental results show that the voltage THD reduction is verified by using the proposed method in the low-speed region and the low-current condition. (see Fig. 10(a)). On the other hand, the characteristic indicates almost same results of the THD either using dual-inverter and single-inverter, at the phase current is 0.2 p.u.

VII. Conclusions

This paper proposes a control method to reduce the voltage harmonics for an OEWIM in the low-speed region. The proposed control method improved the output voltage waveform by using the voltage difference between the dual-inverter and become the modulation index of each inverter was kept high value. This paper introduces the theoretical voltage THD characteristic when using SPVM in the dual-inverter system, which indicates when the motor is driven at low voltage and large PFA, the THD can be reduced by using dual-inverter. The performance of the proposed control method is demonstrated by experiment. This control method allows reducing the voltage harmonics, in particular relates to switching frequency in the low-speed compared with the single-inverter drive. Using proposed method, the voltage THD is reduced by 13.9 %, when the OEWIM is driven at a fundamental frequency of 10 Hz and a phase current of 0.1 p.u.

References

[1] A. Nabae, I. Takahashi and H. Akagi, "A New Neutral-Point-Clamped PWM Inverter," IEEE Transactions on Industry Applications, Vol. IA-17, No. 5, pp. 518-523, Sept. 1981.

[2] M. Morimoto, K. Sumito, S. Sato, K. Oshitani, M. Ishida and S. Okuma, "High efficiency, unity power factor VVVF drive system of an induction motor," IEEE Transactions on Power Electronics, Vol. 6, No. 3, pp. 498-503, July 1991.

[3] K. A. Corzine, S. D. Sudhoff and C. A. Whitcomb, "Performance characteristics of a cascaded two-level converter," IEEE Transactions on Energy Conversion, Vol. 14, No. 3, pp. 433-439, Sept. 1999.

[4] Y. Kawabata, M. Nasu, T. Nomoto, E. C. Ejiogu and T. Kawabata, "High-efficiency and low acoustic noise drive system using open-winding AC motor and two space-vector-modulated inverters," IEEE Transactions on Industrial Electronics, Vol. 49, No. 4, pp. 783-789, Aug. 2002.

[5] S. Chowdhury, P. W. Wheeler, C. Patel and C. Gerada, "A Multilevel Converter With a Floating Bridge for Open-End Winding Motor Drive Applications," IEEE Transactions on Industrial Electronics, Vol. 63, No. 9, pp. 5366-5375, Sept. 2016.

[6] Y. Oto, T. Noguchi, T. Sasaya, T. Yamada and R. Kazaoka, "Space Vector Modulation of Dual-Inverter System Focusing on Improvement of Multilevel Voltage Waveforms," IEEE Transactions on Industrial Electronics, Vol. 66, No. 12, pp. 9139-9148, Dec. 2019.

[7] J. Ewanchuk, J. Salmon and C. Chapelsky, "A Method for Supply Voltage Boosting in an Open-Ended Induction Machine Using a Dual Inverter System With a Floating Capacitor Bridge," IEEE Transactions on Power Electronics, Vol. 28, No. 3, pp. 1348-1357, March 2013.

[8] D. Pan, F. Liang, Y. Wang and T. A. Lipo, "Extension of the Operating Region of an IPM Motor Utilizing Series Compensation," IEEE Transactions on Industry Applications, Vol. 50, No. 1, pp. 539-548, Jan.-Feb. 2014.

[9] Z. Huang, T. Yang, P. Giangrande, S. Chowdhury, M. Galea and P. Wheeler, "An Active Modulation Scheme to Boost Voltage Utilization of the Dual Converter With a Floating Bridge," IEEE Transactions on Industrial Electronics, Vol. 66, No. 7, pp. 5623-5633, July 2019.

[10] Yoshiaki Oto, Toshihiko Noguchi, "Fault-Tolerant Function of DC-Bus Power Source in A Dual Inverter Drive System and Its Operation Characteristics," IEEJ Journal of Industry Applications, Volume 8, Issue 6, Pages 953-959, 2019.

[11] W. Zhao, P. Zhao, D. Xu, Z. Chen and J. Zhu, "Hybrid Modulation Fault-Tolerant Control of Open-End Windings Linear Vernier Permanent-Magnet Motor With Floating Capacitor Inverter," IEEE Transactions on Power Electronics, Vol. 34, No. 3, pp. 2563-2572, March 2019.

[12] Nicolas Denis, Yenyi Wu, Keisuke Fujisaki, "Impact of the Inverter DC Bus Voltage on the Iron Losses of a Permanent Magnet Synchronous Motor at Constant Speed," IEEJ Journal of Industry Applications, Volume 6, Issue 6, Pages 346-352, 2017.

[13] Akihito Mizukoshi and Hitoshi Haga, "Improvement of Output Voltage Waveform in Dual Inverter Fed Open-winding Induction Motor at Low Speed Area," 2018 IEEE Energy Conversion Congress and Exposition (ECCE), pp. 5422-5427, 2018.

[14] Akihito Mizukoshi, Hitoshi Haga, Control Method for Reducing the Motor Loss of Dual-inverter Fed Open-end winding Induction Motor in the Low-speed Region, IEEJ Journal of Industry Applications, 2020, Volume 9, Issue 1, Pages 27-35.

[15] I. J. Smith and J. Salmon, "High-Efficiency Operation of an Open-Ended Winding Induction Motor Using Constant Power Factor Control," IEEE Transactions on Power Electronics, Vol. 33, No. 12, pp. 10663-10672, Dec. 2018.